Nutrient leaching driven by rainfall on a vermiculite clay soil under altered management and monitored with high-frequency time resolution

Barbro Ulén

Published online: 14 Apr 2020.

Submit your article to this journal

Article views: 219

View related articles

View Crossmark data

Taylor & Francis
Taylor & Francis Group

Nutrient leaching driven by rainfall on a vermiculite clay soil under altered management and monitored with high-frequency time resolution

Barbro Ulén 🄳

Department of Soil and Environment, Swedish University of Agricultural Sciences, Uppsala, Sweden

ABSTRACT

Nutrient leaching from clay soils can show extreme temporal and spatial variation. Using an optical sensor (hourly data storage), a Swedish field with vermiculite clay was monitored for water flow (Q expressed in mm), turbidity values (TURB), and nitrate-nitrogen concentrations (CNO_3N, mg L^{-1}) in four hydrological years representing different cropping/soil management regimes. Mean TURB-Q slope (1300) decreased in the order: ploughed soil > winter wheat > unfertilized fallow > winter wheat after drainage system renovation + structure-liming of topsoil and backfill, estimated in the initial phase from 16 selected autumn events. A similar ranking was found for variability in turbidity relative to that in discharge (CV_T/CV_Q) in the entire autumn. Mean CNO_3N-Q slope (=2) was significantly lower under fallow than in the three cropping systems (7-32), confirming results from adjacent experimental plots. A spring-period had no snow cover or intensive rain, but *in situ* monitoring revealed that nutrient leaching was still substantial. Particulate- and dissolved reactive phosphorus, and nitrate-nitrogen leaching was estimated reasonably well (less than 8% difference) based on *in situ* high-frequency resolution measurements, compared with laboratory analysis of weekly composite samples. Accurate assessment of *C-Q* relationships in agricultural drainage water across temporal and spatial scales is therefore important.

Introduction

A prerequisite for crop production in Nordic agriculture is artificial drainage of fine-textured soils. Drainage changes soil hydrology and water flow (Q), and is commonly reported to cause less erosion and reduced phosphorus (P) losses, but increased nitrogen (N) leaching (Gramlich et al. 2018). Soil clay content has long been suggested to be an important explanatory factor for soil erosion and associated P losses, and for dissolved P concentrations, due to adsorption/desorption (e.g. Ryden et al. 1974). However, for soils with a high content of vermiculite, and hence with a structure of interlayered hydroxyl-aluminum, desorption of P is mainly a function of ligand exchange by the phosphate molecules within these layers (Penn et al. 2005). Thus it is important to consider clay mineralogy in assessments of P losses from fine-textured soils. Additionally, ammonium (NH_4^+) ions are known to be fixed within the interlayer space of vermiculite, which suppresses denitrification and thereby limits leaching of nitrate-nitrogen (NO_3N) (e.g. Scherer 1993). Any NO_3 present is less efficiently trapped and even bedrock N, especially

in the form of weathered slate, may significantly contribute to high NO_3N concentrations in water (Holloway et al. 1998).

Using different indices, previous studies have identified topsoil as the dominant source of P in tile-drained clayey soils with preferential flow as the dominant pathway. For example, it has been shown that strongly sorbed P appears at the same time as more or less weakly sorbed substances (Flury 1996) and that particulate P (PP) concentrations are clearly related to a range of pesticides representing both low and high sorption ability (Ulén et al. 2014) Additionally, X-ray diffraction has revealed a similarly high degree of hydroxyl-aluminum interlayering and high total organic carbon concentrations in particles collected from drainage water and topsoil particles (Simonsson et al. 2019).

Effects of mitigation measures aimed at reducing leaching of dissolved reactive P (DRP), P in other forms (e.g. PP), and NO_3N are difficult to identify, since the outcomes may be masked by annual weather conditions and climate change and since assessment is problematical even with a rigorous flow-adapted experimental set-

CONTACT Barbro Ulén ✉ barbro.ulen@slu.se 📧 Department of Soil and Environment, Swedish University of Agricultural Sciences, PO Box 7014, Uppsala SE-750 07, Sweden

up (Ulén et al. 2018). The effects are also obscured by hysteresis effects commonly observed in nutrient concentration–discharge (C–Q) relationships (e.g. Lloyd et al. 2016a). Sensor techniques may be useful for mass balance calculations, but must first be carefully assessed, particularly at small spatial scales, since most previous monitoring studies using high-frequency time resolution have focused on streams, rivers, or lakes, rather than agricultural fields. Temporal variations in C–Q relationships may lower the accuracy of leaching estimates based on flow-proportional water samples, but does not affect that of measurements based on optical sensors. On the other hand, only a limited number of different forms of N and P can be monitored at a reasonable cost using optical sensors.

It has been suggested that the ratio of coefficient of variation in concentration to that in discharge (CV_c/CV_Q) can be used as an index for partitioning between 'chemodynamic' and 'chemostatic' state (Thompson et al. 2011). A value of 1 can represent either a dilution or enrichment response, which can be confirmed by regression between C–Q slope and CV_c/CV_Q (Zimmer et al. 2018). This index has been tested on rivers and streams, but rarely in small-scale areas and never previously for an agricultural soil-water system with a low level of legacy P.

Most published studies on C–Q variability cover a few events or a few years (e.g. Kämäri et al. 2018) and there is still little knowledge about differences and similarities between event-scale and more long-term C–Q relationships. Seasonality in the C–Q relationship has been found to be diverse or unclear (Knapp et al. 2020). In a cold-climate river, the C–Q relationship has been demonstrated to be affected by snow accumulation and dilution of NO_3N relative to Q (Kämäri et al. 2018). In order to avoid ambiguities in annual solute response to Q, winter months may be excluded, e.g. in a study of a relative small forest catchment by Knapp et al. (2020). With better availability of comprehensive and detailed climate and soil hydrological data, C–Q variability could be more accurately determined.

This study complements previous work in which yearly P leaching from an artificially drained field was studied using composite samples from mixed flow-proportional subsamples (Ulén et al. 2018). Soil mineralogy in the observation field is dominated by vermiculite with high potential to sorb P. In the present study, a set of clear hydrological events was selected for description of event-response dynamics to multi-mitigation measures aimed at reducing P leaching. The selection was limited to clear Q events with potential to be repeatable from year to year. Since base-flow is unclear in small streams and ditches that regularly dry out in summer droughts and winter frosts, the assessment

was limited to the rising limb of events in autumn and when pre-storm events suggested wet soil.

The aims of the study were to:

(i) Quantify event-scale C–Q pattern, C/Q variability, and load of in situ-measured turbidity and NO_3N in four consecutive autumns from a drained agricultural field under altered management.
(ii) Quantify Q, C/Q variability (turbidity and NO_3N), and transport of several forms of N and P in entire autumns, and corresponding variables covering the hydrological years, based on flow-proportional water techniques.
(iii) Quantify event-scale precipitation-discharge, C–Q pattern, C/Q variability, and load of in situ-measured DRP in a pilot study covering a period of high soil moisture after snowmelt.

The hypothesis tested was that turbidity and NO_3N concentration slopes can direct P and N leaching under altered farm and soil management.

Materials and methods

Studied field

The observation field (4.2 ha) is situated in Oxelby, 15 km south of the city centre of Stockholm, Sweden (Figure 1), and it drains to Lake Bornsjön, the reserve drinking water reservoir for the city. The climate is characteristic of the Nordic region, with mean monthly temperature varying from −3.0°C in February to 17.2°C in July and mean annual precipitation of 540 mm (reference period 1961–1990) (SMHI 2019). Land elevation at the site is 15 m a.s.l. The soil is mainly clay, with the highest clay content in the lower central part of the field, bordering an experimental area. The clay is strongly dominated by vermiculite (M. Simonsson, pers. comm. 8 June 2019). Soil P status (analysed according to Egnér et al. 1960) is spatially variable (mean 70 mg kg^{-1} P-AL in 2006), with low concentrations in the main lower part of the field and higher concentrations in the upper part (Ulén et al. 2018). The soil has been artificially drained, probably for more than 50 years, to provide essential drainage. The collection pipe of single or paired tail drains ends at an open ditch, to which the water is pumped. The field was cropped with winter wheat in 2010/2011, spring barley in 2012, fallow in 2012/2013, and winter wheat in 2013/2014, except for a minor plot area with other crops in 2011–2012. Soil tillage was moderate in the four-year study period (October 2010–September 2014). Shallow incorporation of winter wheat residues was performed with a cultivator
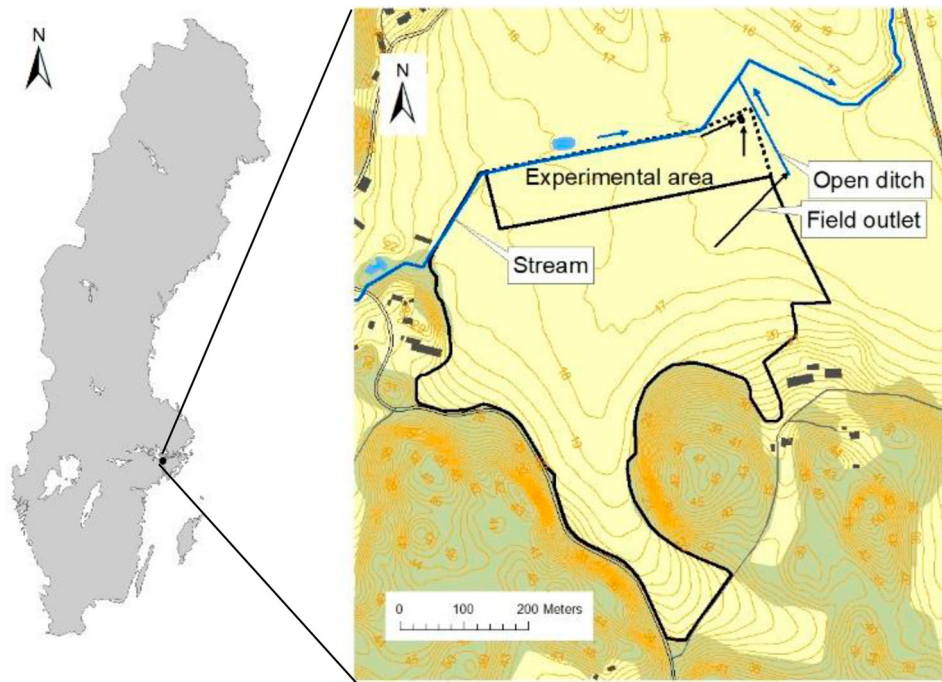
Figure 1. Location and topography of the Oxelby field. An experimental area with a separate outlet to the ditch is situated just north of the field.

in early autumn 2011 but, due to problems with volunteer plants, the soil was ploughed and tilled in late autumn 2011. Only small amounts of mineral P fertiliser have been applied over the past 30 years, since P application is restricted in the area. In the study period, the field received 9–10 kg P ha^{-1} in mineral form on two occasions (17 May 2012 to barley and 15 April 2014 to wheat). Nitrogen fertilisation at a moderate rate (mineral form) also took place each spring (late April–early June) except in 2013, when the field was left unfertilised under fallow. In August 2013, the entire field area was structure-limed with a commercial mixture containing 18% 'active' calcium hydroxide in the form of slaked lime [Ca(OH)$_2$] at a rate equivalent to 1 ton 'active' CaO ha^{-1}. The lime mixture was applied in dry weather on the cut fallow and was immediately incorporated evenly into the topsoil with two passes of a cultivator in different directions to simultaneously break up the fallow and incorporate it. Three weeks later, the drainage system was renovated with drainage pipes placed in a herring-bone pattern at 14 m spacing (0.07 m^{-2}) in the entire middle and lower part of the field (two-thirds of the area) with accompanying soil digging. The uppermost one-third of the field was left without drain renovation. Gravel (4–8 mm) was placed in the bottom of the drains, which amounted in total to 15,375 linear metres. Structure lime containing 18% active CaO, equivalent to 1.2 kg CaO m^{-1}, was incorporated into the soil used as backfill above the drains in the central part of

the field (one-third of the field area). The backfill in the lowest part of the field (one-third of the field area) was treated with higher intensity and received double the amount of structure lime.

Water monitoring

Precipitation and air temperature were measured close to the field outlet and snow cover was recorded in another field (Norsborg) 7 km from the site (SMHI 2019). Water discharge was measured in a concrete basin in a monitoring cabin, where Q was gauged continuously through an open V-notch weir (90°), with the water level calibrated to a displacement body acting as a float and hanging in a load cell connected to a datalogger.

Automated measurements of NO$_3$N and turbidity were performed with an optical sensor (s::can nitro:lyser Messtechnik, GmbH) from October 2010 until the sensor broke in a thunderstorm on 29 July 2014. The sensors were placed in the concrete basin just below the V-notch weir and at the same level as the inlet for an autosampler. Sensor measurements were based on absorbance in the UV-visible range (200–750 nm) with measuring range 0–100 mg L^{-1} NO$_3$N and 0–1000 formazin turbidity units (FTUS). Before each measurement, the window of the sensor was cleaned with compressed air. The instrument was manually checked and cleaned at least once every six months and the baseline was regulated. Concentrations of NO$_3$N (CNO$_3$N) and turbidity

values (TURB) were estimated from the corrected value of absorbance. Mean hourly values were calculated and stored hourly by the datalogger. Turbidity and CNO_3N were also calibrated for TURB and NO_3N from manual water sampling. In the period 16 March–3 April 2012, concentrations of dissolved reactive P (CDRP) were measured with Systea Micromac 1000 (SYSTEA S.p.a, Anagi (FR), Italy) after pre-filtration through a filter (pore diameter of 25 µm), which was cleaned by compressed air from the nitro::lyser. Measurements of CDRP, which included blank and calibration, were carried out hourly and the concentration values were stored internally by the instrument.

Flow-proportional sampling of drainage water took place weekly or bi-weekly. Weekly sampling was performed in the test period in spring 2012 and in other periods when leaching was most intensive. Each flow-proportional subsample represented 0.15 L m^{-2} corresponding to 1–2 subsamples per hour in peak flows. Composite water samples were collected in 10-L glass vessels, stored at approximately 10–14°C in darkness. Representative subsamples were sent in 100-mL glass bottles for chemical analysis at the Water Laboratory at the Department of Soil and Environment, SLU. Dissolved reactive P (DRP) was analysed (ECS 1996) within two days after storage at +4°C, following pre-filtration using filters with pore diameter 0.2 µm (Schleicher & Schüll GmbH, Dassel, Germany). Total P (TP) was analysed within four days after storage at +4°C as reactive P after acid oxidation with $K_2S_2O_8$ (ISO 2003). Particulate P (PP) was estimated as the difference between TP in filtered and unfiltered samples. Turbidity was determined immediately after shaking the sample, using a turbidimeter (Hach-Lange Company, Düsseldorf, Germany). Concentration of ammonium-N (CNH_4N) was analysed according to ISO (2005). Nitrate-nitrogen and nitrite-nitrogen were analysed together (ISO 1996) and referred to as NO_3N, since the concentration of nitrite-nitrogen was found to be negligible. Total organic carbon (TOC) was analysed together with total nitrogen (TN), using a CN analyser (Shimadzu).

Data analysis: estimations and statistics

Only rainfall-driven Q events in autumn (October–December) were assessed, since snow cover varied greatly between the winters and since distinct Q events rarely appeared in two of the monitored summers. In autumn, the simplest events without a nested pattern of the TURB-Q and CNO_3N-Q relationships were selected. The initial phase was defined as when Q reached its peak and only this phase was assessed, since the endpoint of the events was more difficult to define than the starting time. A second selection criterion was for an approximately linear relationship between TURB and Q (and

also between CNO_3N and Q), with an adjusted coefficient of determination (r^2_{adj}) of at least 0.75 as the condition. Hourly increase in Q was estimated as dQ/Q for the short initial periods of Q events, and for the entire autumns. Variability in C–Q was expressed as CV_c/CV_Q according to Thompson et al. (2011) for the same initial parts of the events and for the entire autumns and hydrological years. The slopes of TURB-Q and CNO_3N-Q were estimated from the regression lines. Selected events (initial phase) were also characterised by the amount and maximum intensity of rain that fell within events, or at most one day previously.

Non-rainfall and rainfall-driven events in March-April 2012 were observed for hysteresis towards Q, together with the C–Q relationship for NO_3N and DRP. Concentration of PP (CPP) was estimated based on the sensor turbidity values and from linear regression (r^2_{adj}, 0.87) of CPP versus TURB (range 0–200 FTUs and 0.04–0.29 mg PP L^{-1}) based on manual sampling in the same period. Nutrient leaching was estimated from hourly values from the sensor and DRP analysed *in situ*. In parallel, nutrient leaching was estimated from the composite samples made from the flow-proportional subsamples.

All statistical analyses were performed in MINITAB and comparisons were made using t-test, with $p < 0.05$ indicating statistical significance.

Results

Precipitation and water discharge in autumn events

The hydrological year 2010/11 started wet after several intensive rain events in the previous summer. This autumn period with repeated rain was shorter than in the following three autumns, since permanent snow cover appeared in early December 2010 and in late December/early January in the following years. Winter conditions with permanent snow cover also lasted unusually long in spring 2011 (until early April), but snow-melt conditions occurred several weeks earlier in the following springs. Additionally, the relatively short snow cover in January-early March was interrupted by one or two melting periods in between. In spring 2012, the period between last snowmelt (7 March) and first more intense rain (28 March) lasted three weeks.

Selected autumn events (four per year) are marked in the autumn hydrographs shown in Figure 2(a–d). These events were induced by 2–16 mm rainfall with maximum intensity 0.4–3.8 mm h^{-1} on days 15–77 from the beginning of the hydrological year (Table 1). The initial phase lasted for 5–11 h, during which Q was 0.2–2.4 mm h^{-1}, with a mean increase (dQ/Q) from 0.1

to 0.7. None of the means of these parameters differed significantly between the four autumns. Water discharge in these 16 events represented on average 3% of total Q in October–December.

Turbidity and NO₃N concentrations in selected autumn events

The hysteresis loop for the relationship between turbidity and Q was commonly clockwise and the value reached its maximum one hour before the Q peak. Two typical examples are given in Figure 3 (2 December 2011) and Figure 4 (5 November 2013). Exceptions were the two first events (not included in Table 1) after the dry summer of 2013, following which the drainage system was renovated. The loops were anti-clockwise and turbidity reached its peak one hour after the

drainage peak. The hysteresis loop for the relationship between CNO_3N and Q was always anti-clockwise, and the value reached its maximum one or two hours after the Q peak. Nitrate-N event concentration was generally low in all autumns, but during the third rain event after drainage system renovation it rose from 1 to 19 mg L^{-1} and remained high in all subsequent events. The ratio of variability in TURB to variability in Q (CV_T/CV_Q) was commonly >1, while that for CNO_3N (CV_N/CV_Q) was <1, with the single exception of the second event in autumn 2013 (Table 1). Regression lines between C–Q slope and CV_T/CV_Q or CV_N/CV_Q were generally non-significant, but a significant positive trend was seen in some individual autumn periods (TURB in 2012 and CNO_3N in 2010 and 2013).

Mean TURB-Q slope (1300) decreased in the order: ploughed soil > winter wheat > unfertilised fallow >
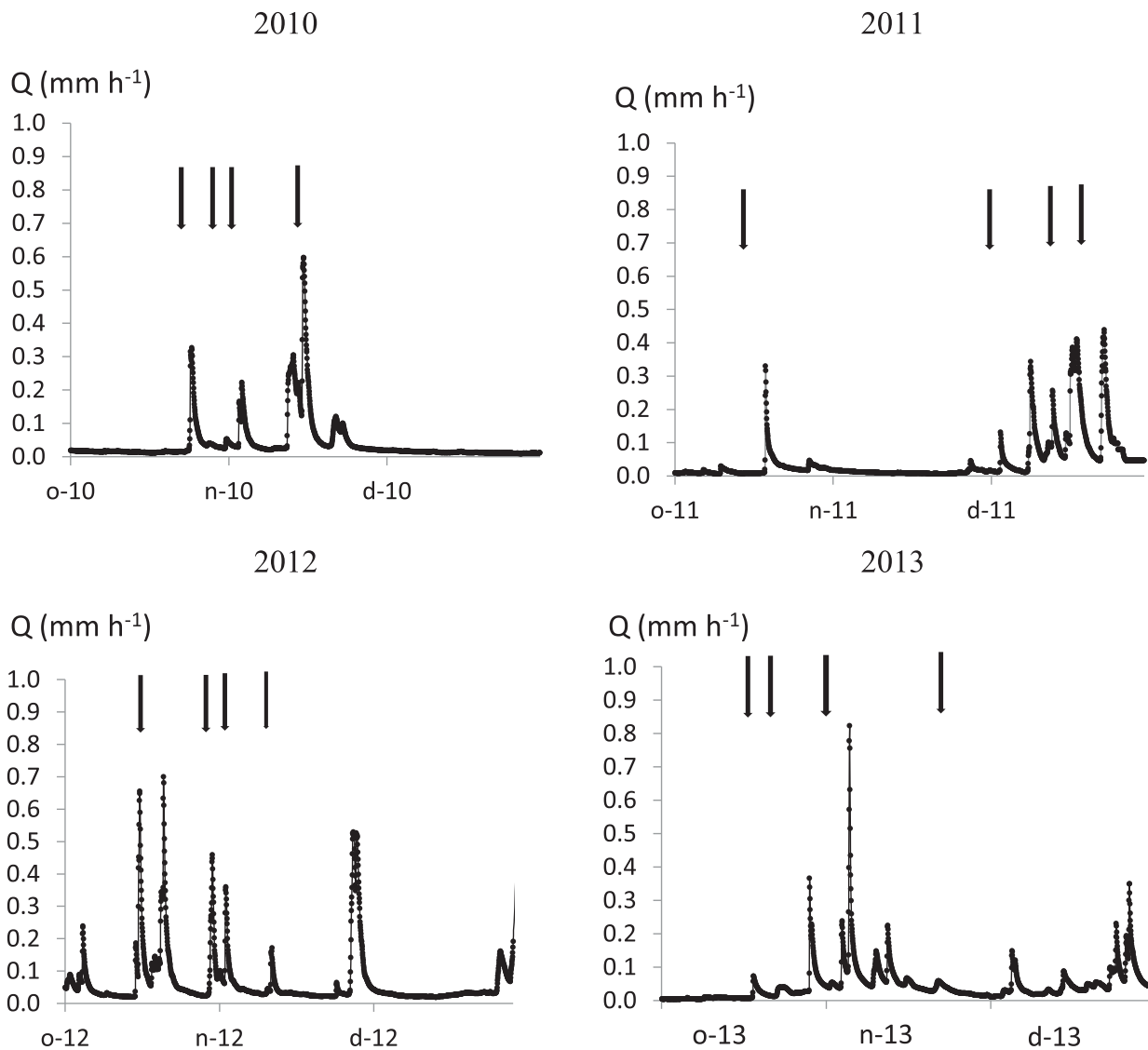

Figure 2. Autumn (October–December) hydrograph 2011–2014, with selected events marked with arrows.

Table 1. Autumn event day (D) since 1 October, maximum intensity (Max), amount (R) of rainfall, mean increase (dQ/Q) and amount (Q) of discharge until peak, flow-weight mean turbidity value (C), with hourly increase (Rate) and with slope to Q, and variability related to Q (CV_T/CV_Q) and corresponding parameters for nitrate-nitrogen concentration (CNO_3N) (Rate) and slope and variability to Q together with yearly means ($\dot{X}$) of all parameters under different cropping/soil management regimes

D	Rainfall		Discharge		TURBIDITY				NO$_3$N			
	Max (mm h^{-1})	R (mm)	dQ/Q –	Q (mm)	C (FTU)	Rate (dC h^{-1})	Slope –	CV_T/CV_Q	C (mg L^{-1})	Rate (dC h^{-1})	Slope –	CV_N/CV_Q
Autumn 2010 *Winter wheat sown in September*												
25	2.8	9.4	0.31	0.27	90	24	860	0.8	2.6	0.26	9.1	0.6
31	1.2	3.6	0.11	0.23	110	27	630	2.1	1.1	0.04	12.0	0.7
33	1.6	4.8	0.27	0.54	200	60	2900	1.3	1.5	0.19	6.9	0.6
46	0.4	2.2	0.23	1.37	290	67	840	0.9	2.1	0.12	1.3	0.5
$\dot{X}$	1.5	5.0	0.23	0.60	170	45	1800[a]	1.3	1.8[a]	0.15[ab]	7.3[ab]	0.6
Autumn 2011 *Volunteer plants with late (3th December) ploughing*												
18	3.4	13.4	0.38	0.96	420	91	2200	1.0	3.4	0.60	9.0	0.6
64	2.6	3.6	0.72	0.29	150	43	2600	1.0	3.0	0.45	16.3	0.5
74	2.6	3.8	0.16	0.52	70	56	1500	1.4	4.4	0.11	10.9	0.3
77	1.6	3.4	0.06	0.73	180	43	2600	1.8	4.5	0.23	20.8	0.5
$\dot{X}$	1.6	6.1	0.33	0.63	210	58	2200[ab]	1.3	3.8[b]	0.35[b]	14.2[ab]	0.5
Autumn 2012 *Unfertilised fallow*												
15	2.8	15.6	0.16	2.99	410	43	700	0.9	1.6	0.10	1.6	0.5
30	1.0	7.2	0.19	0.89	100	14	580	0.9	1.4	0.09	1.7	0.2
32	1.4	3.0	0.30	0.98	240	66	950	1.0	1.4	0.11	1.4	0.5
41	1.4	4.6	017	1.04	260	40	2000	1.2	0.8	0.03	4.2	0.8
$\dot{X}$	1.3	7.6	0.21	0.31	230	41	1100[ac]	1.0	1.3[a]	0.08[a]	2.2[ac]	0.5
Autumn 2013 *Winter wheat after drainage system renovation + structure liming*												
28	2.8	10.0	0.19	0.87	200	46	610	0.7	18.9	2.61	37.4	0.5
34	2.2	6.0	0.22	0.87	70	15	260	6.4	19.8	3.52	50.7	1.1
36	2.2	9.3	0.30	2.43	160	24	320	0.8	16.3	3.21	10.8	0.2
66	0.8	4.0	0.49	0.74	50	8	11	0.7	18.8	1.43	27.8	0.3
$\dot{X}$	2.0	7.3	0.30	1.23	120	23	300[ac]	2.1	17.2[c]	2.89[c]	31.7[ab]	0.5

Note: Mean values with different letters (a, b, c) are significantly different ($p < 0.05$).

winter wheat after drainage system renovation + structure-liming of topsoil and backfill. The difference was significant between the ploughed soil in autumn events 2011 and the fallow (autumn events 2012), and also between the ploughed soil 2011 and the managed soil 2013 (Table 1). In contrast, there was no significant difference in turbidity, or CV_T/CV_Q, when comparing events representing different farm and soil management measures.

Mean CNO_3N-Q slope was significantly lower under fallow (mean = 2) than under the three cropping systems (range = 7–32). The difference in CNO_3N-Q slope was especially apparent when comparing episodes in the autumn under fallow with episodes in the following autumn after terminating the fallow and improving the drainage (Table 1). Significant differences were also estimated for CNO_3N and for the absolute rate of change in NO_3N concentration ($dCNO_3N$ h^{-1}) (Table 1).

a)

TURB (FTUs)

b)

NO$_3$N (mg L^{-1})

Figure 3. Example of hysteresis curve for hourly (a) turbidity (TURB) and (b) concentrations of nitrate-nitrogen (CNO_3N) in a rain-driven event on 2 December 2011. The soil was under winter wheat.
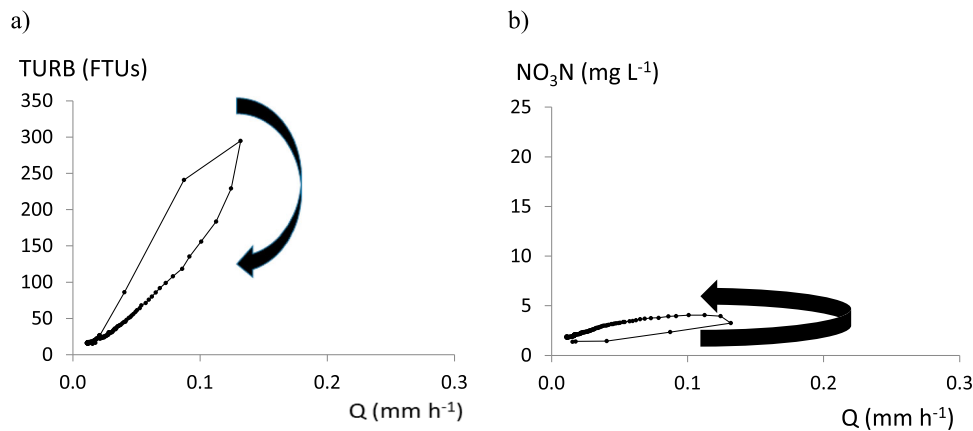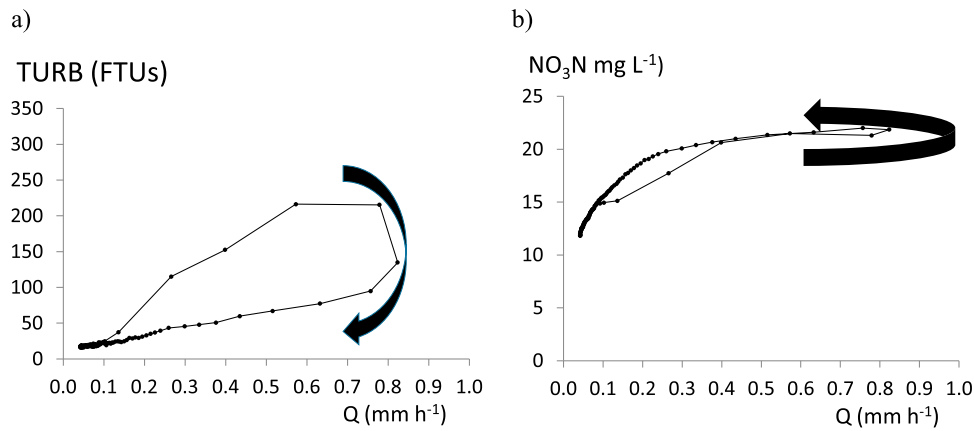
Figure 4. Example of hysteresis curve for hourly (a) turbidity (TURB) and (b) concentrations of nitrate-nitrogen (CNO$_3$N) in a rain-driven event on 5 November 2013. The soil was under winter wheat after drainage system renovation and structure-liming of topsoil and drain backfill.

Turbidity, N, and P concentrations in entire autumns and hydrological years

Both turbidity and suspended solids (SS) concentrations were higher in autumn than in the entire year in the first three years (Table 2). With snowmelt and thawing in spring, dilution of particle and soil colloid concentrations in drainage water seemed to occur. The ranking of the autumn CV_T/CV_Q and the event TURB-Q slope for farm management measures was ploughed soil > winter wheat > unfertilised fallow > winter wheat after drainage system renovation + structure-liming of topsoil and backfill, while the ranking between turbidity and SS for farm management was inconsistent.

In total, *in situ* measurement of NO$_3$N resulted in 15% higher flow-weighted mean concentrations than laboratory measurements on subsamples. The difference was largest in the last year of the study period (Table 2). Monthly calibration of sensor values is desirable (Ulén et al. 2019), and might have reduced this difference. The CV_N/CV_Q value was rather low (0.2–0.6) compared with CV_T/CV_Q (0.4–0.1). A feature typical for the study site was the nearly negligible concentrations of NH$_4$N in drainage water. Presence of organic forms of N, estimated as the difference between total N and mineral N, was only apparent in the autumns with winter wheat and that with fallow.

Phosphorus concentrations, PP concentrations, in particular, were lower in 2013/2014 than in the other three years (Table 2). Particulate P related to SS concentration was 0.11–0.33% in autumns and 0.41–0.47% in entire years, with the highest proportion in the last year after improved drainage and liming (Table 2).

Table 2. Discharge (*Q*) (mm) and flow-weighted mean concentrations of turbidity (FTUS), suspended solids (SS), total organic carbon (TOC), and nutrients (mg L^{-1}), with nitrate-nitrogen measured either *in situ* (NO$_3$N$_{in\ situ}$) or in laboratory-analysed composite samples from flow-proportional subsamples (NO$_3$N$_{flprop}$) in autumn (October–December) and in hydrological years (Hydyear: October–September). Turbidity variability relative to *Q* (CV_T/CV_Q) and corresponding parameter for NO$_3$N (CV_N/CV_Q).

Period	Autumn 2010	Hydyear 2010/11	Autumn 2011	Hydyear 2011/12	Autumn 2012	Hydyear 2012/13	Autumn 2013	Hydyear 2013/14[a]
Q	98	284	105	474	175	348	109	252
TURB $_{in\ situ}$	130	60	130	95	120	80	15	40
SS$_{flprop}$	340	190	320	200	310	160	22	40
NO$_3$N$_{in\ situ}$	1.5	2.1	4.3	4.2	1.2	1.3	9.4	8.2
NO$_3$N$_{flprop}$	1.3	2.2	4.2	3.9	1.2	1.0	8.3	7.0
NH$_4$N$_{flprop}$	0.03	0.03	0.01	0.01	0.01	0.01	0.01	0.01
TN$_{flprop}$	2.1	2.3	5.4	4.7	1.7	1.2	9.8	7.1
TOC$_{flprop}$	11.0	6.6	9.7	7.3	7.5	5.1	4.8	4.4
PP$_{flprop}$	0.52	0.26	0.31	0.21	0.36	0.19	0.04	0.05
DRP$_{flprop}$	0.07	0.07	0.05	0.05	0.05	0.03	0.02	0.02
TP$_{flprop}$	0.61	0.35	0.38	0.27	0.41	0.22	0.09	0.09
CV_T/CV_Q	0.80	1.01	0.87	0.79	0.69	0.80	0.41	0.47
CV_N/CV_Q	0.30	0.36	0.59	0.50	0.09	0.19	0.24	0.36

[a]The sensor broke in a thunderstorm on 29 July.

Turbidity, NO$_3$N, and DRP concentrations after snowmelt in spring 2012

In spring 2012, no precipitation fell on the soil in the period 16–28 March. In the same period, discharge from the warming and thawing soil was substantial (8 mm), but with a very moderate increase in rate (dQ/Q < 0.01) compared with in autumn events (dQ/Q = 0.1–0.5). Both TURB and CNO$_3$N were approximately synchronised with Q (Figure 5), but CDRP-Q demonstrated extended clockwise hysteresis most of the time. The slope of the TURB-Q curve (200) was only one-tenth of the value in autumn before the soil was ploughed, while both CNO$_3$N and the CNO$_3$N-Q slope were similar.

After a few mostly minor rainfall events (Table 3), concentration loops with complex hysteresis followed. Dissolved reactive P concentrations were similar in the period 28 March–4 April and in the preceding period (mean 0.04 mg L^{-1}), but TURB was significant higher in 28 March–4 April (mean 38) than in the later period (mean 28), when the discharge amount was three times less than that in the non-rainfall period.

Nutrient leaching in events, in spring 2012, and in entire years

The leached amounts of particles, measured as turbidity in the selected events (Table 1), represented a minor proportion (4%, 4%, 9%, and 18%, respectively) of total leached turbidity in autumn 2010–2013. The leached amounts of NO$_3$N in the same events represented 3%, 2%, 3%, and 15%, respectively, of the leached amounts of NO$_3$N in the four autumns. Nitrate leaching was highest in the last year, especially in the autumn, and lowest in the year with fallow (2012/2013). High NO$_3$N leaching was still observed in the year after break-up of fallow/drainage system renovation, but leaching was moderate in the following year (data not shown). On a yearly basis, leaching of organic N represented 5%, 21%, 20%, and 1% of total leaching in 2010–2014. Leaching of TOC was generally low, giving a low C/N ratio. After structure liming, this ratio was even <1.

Particulate phosphorus, DRP, and NO$_3$N leaching in the 18-day monitoring period in spring 2012 was estimated reasonably well (less than 8% difference) based
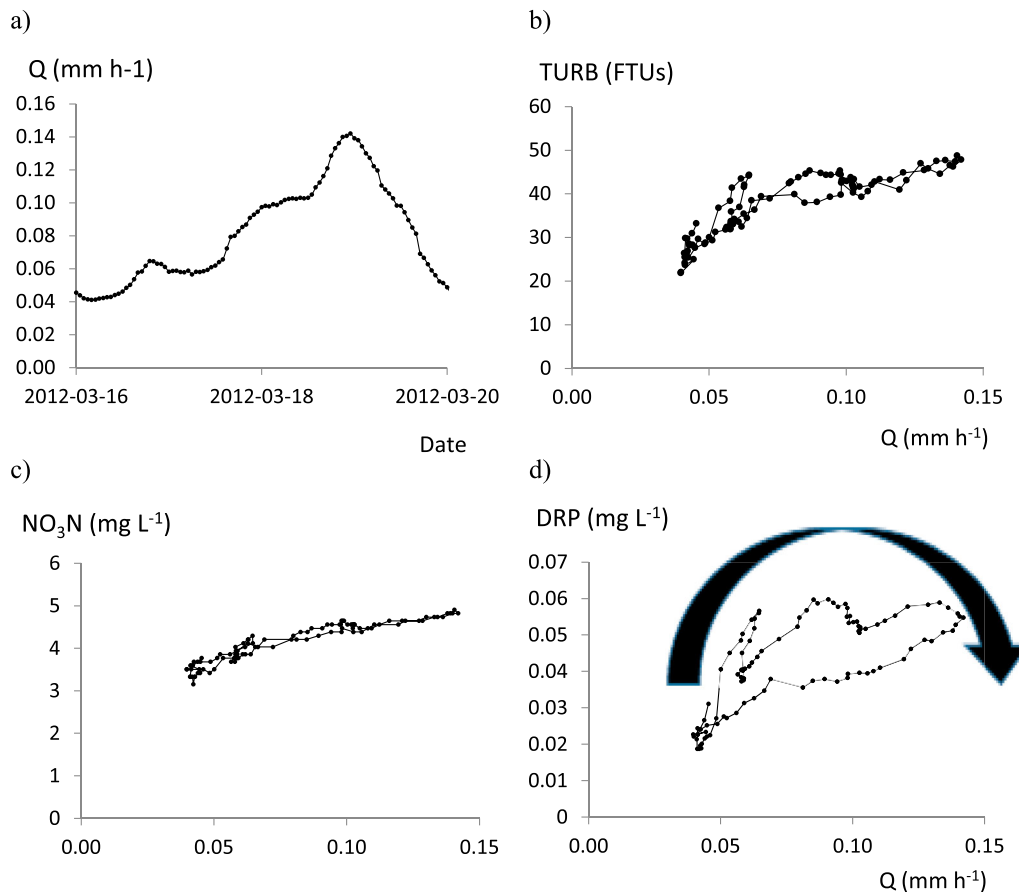

Figure 5. (a) Hourly discharge (Q, mm), hysteresis curve for hourly (b) turbidity and (c) concentration of nitrate-nitrogen (NO$_3$N), and (d) concentration of dissolved reactive phosphorus (DRP) in a non-rain period when the soil was thawing in spring 2012.

Table 3. Mean air temperature (Temp), sum of rainfall (Rain), mean increased (dQ/Q) and amount of discharge (Q), flow-weight mean turbidity (TURB) values, with mean slope to Q and turbidity variability related to Q (CV$_T$/CV$_Q$), and corresponding parameter nitrate-nitrogen (NO$_3$N) and dissolved reactive phosphorus (DRP) in a spring period without rain (No-rain) followed by a period with some rainfall (Rain).

	Two spring periods after snowmelt 2012	
	16–20 March	28 March–4 April
Parameter	No-rain	Rain
Air temp (°C)	3.8	2.4
Rain (mm)	0	5.6 + 2.0 + 4.0 + 0.6
dQ/Q	0.006	0.005
Q (mm)	8.2	2.7
TURB (NTUs)	38	28
Slope TURB-Q	200	–
CV_T/CV_Q	0.5	1.5
CNO$_3$N (mg L^{-1})	4.1	3.2
Slope CNO$_3$N-Q	14	–
CV_N/CV_Q	0.3	0.3
CDRP (mg L^{-1})	0.04	0.04
Slope C$_{DRP}$-Q	0.30	–
CV_P/CV_Q	0.8	1.0

Table 4. Nutrient leaching (g ha^{-1}) based on *in situ* analysis (Systea Micromac 1000) and laboratory analysis of composite samples collected weekly (Flow-prop. subsampling) and measured by optical sensors in an 18-day study period in spring 2012.

Nutrient		Monitoring technique	Leaching
Dissolved reactive phosphorus	(DRP)	Systea Micromac 1000	8.2
Dissolved reactive phosphorus		Flow-prop. subsampling	8.4
Particulate phosphorus	(PP)	Optical sensor[a]	18
Particulate phosphorus		Flow-prop. subsampling	20
Total phosphorus	(TP)	Flow-prop. subsampling	29
Nitrate nitrogen	(NO$_3$N)	Optical sensor	890
Nitrate nitrogen		Flow-prop. subsampling	825
Ammonium nitrogen	(NH$_4$N)	Flow-prop. subsampling	0.07
Total nitrogen	(TN)	Flow-prop. subsampling	850
Total organic carbon	(TOC)	Flow-prop. subsampling	960

[a]Based on monitoring of turbidity and regression between PP and turbidity (grab samples).

on *in situ* high-frequency resolution measurements compared with when based on laboratory analysis of weekly composite samples (Table 4). In the four-year study, DRP was 11–24% of TP leached, characteristically with a higher proportion in spring than autumn. In spring 2012, with thawing soil, DRP was 28–29% of TP leached.

Discussion

Hysteresis and impact of hydro-climatological factors

The present study revealed clockwise hysteresis in CDRP-Q, which is often associated with rapid DRP displacement from the surface or near-surface (e.g. Eludoyin et al. 2017). However, particles settling in tile drains and in the measuring container, and then easily transported in high-flow events, could also have contributed. This is supported by the finding that no such hysteresis was observed when the tile drains were replaced during renovation. In contrast, the relationship between CNO$_3$N and Q was always anti-clockwise. Anti-clockwise loops generally indicate a lag between concentration and discharge, e.g. from a source located far away with longer travel time. In catchment studies, anti-clockwise hysteresis of CNO$_3$N has therefore been suggested to depend on a significant contribution from tile drain systems (e.g. Bauwe et al. 2015) and hysteresis analysis has been suggested for characterising their likely contribution to some areas. Anti-clockwise curves with NO$_3$N in urban watersheds have also been interpreted as representing dilution in the initial phase ('first flush' effect) (Duncan et al. 2017). At our study site, with extremely fast water infiltration into the soil (Svanbäck et al.

2014), a possible explanation for the anti-clockwise NO$_3$N hysteresis loop could be that more NO$_3$N is delivered by the rising groundwater soon after rainfall.

In the present study, the variability in nutrient concentrations relative to that in Q (CV$_C$/CV$_Q$ ratio) was tested as an index of partitioning between transport-dominated and chemostatic behaviour. The value for turbidity (CV$_T$/CV$_Q$) was commonly >1, while the corresponding value for CNO$_3$N (CV$_N$/CV$_Q$) was less than 1 (Table 2), demonstrating the importance of particle transport for P leaching. With the first rain falling on the soil after snowmelt in spring 2012, CV$_T$/CV$_Q$ rose from 0.5 to 1.5. This reflects the fact that rainfall adds energy to the soil, while soil thawing is a more gentle and gradual process.

Different combinations of hydro-climatological conditions influence the hysteresis pattern for each particular hydrological event, while antecedent hydroclimatological factors may also exert an influence (Blaen et al. 2017). For classification and assessment of hysteresis at a given site, the number of hydro-climatological factors considered must be balanced against the number of clear events montored. In a small-scale, short-term (14-month) study by Liu, Youssef, et al. (2020), all events with a minimum of just three data points on the rising limb were included in the assessment of nine different hydrological factors. The number of events (22) was large, however, since irrigation took place in the drained agriculture field.

The feature of the hydrograph for a network of small pipe-lined subsurface drains (artificial drainage systems) depends on a complex range of factors. In such systems,

Q fluctuations are expected to be even more varied than in natural running waters. Hydrological events are commonly designated in relatively simple terms, such as duration, maximum Q, and time to last storm (e.g. Eludoyin et al. 2017). However, recent C–Q studies have included directly monitored factors and hydrological indices, to allow more careful assessment of the hydrological events and antecendent conditions affecting the C–Q relationship. Shallow groundwater levels and soil moisture content were recorded at high frequency, along with air temperature and precipitation, in a study by Blaen et al. (2017). High-frequency measurements of shallow groundwater levels were combined with a simple base-flow index in another large agricultural catchment (Outram et al. 2016), but a base-flow index is less applicable in small streams and ditches that regularly dry out in dry summers and cold winters. Blaen et al. (2017) concluded that wet antecendant conditions, together with precipitation intensity, are key drivers in hysteresis of NO_3N and dissolved organic carbon (DOC). Dry antecendant conditions have been demonstrated to have an effect in temporary enhancement of NO_3N and TP loads (Outram et al. 2016) and have also been estimated to have an impact on NO_3N hysteresis (Liu, Youssef, et al. 2020).

In order to specify the direction and strength of the hysteresis relationship, a hysteresis index (HI) based on concentration after flow-normalisation has been suggested (Lloyd et al. 2016b). A 'flushing index' (FI), which combines flushing and dilution, has also been suggested (Vaugham et al. 2017). Both indices, with value ranging from −1 to 1, were included in an assessment of NO_3N dynamics in drainage water at the edge of a small irrigated site with pasture (Liu, Youssef, et al. 2020), together with an advanced experimental setup for monitoring CNO_3N at three different depths and distances from the drain pipe (Liu, Maxwell, et al. 2020). Those studies demonstrated a significant correlation between HI and the initial Q in events, while the statistical assessment revealed a more complicated influence of FI that covered several factors. Moreover, CNO_3N in groundwater varied spatially depending on the position of the drainge pipes (Liu, Youssef, et al. 2020; Liu, Maxwell, et al. 2020).

Concentrations and leaching under altered management

The low SS concentration and turbidity in autumn 2013 in the present study indicate effects of drainage and soil management. Intensive soil management practices have also been suggested to reduce PP leaching measured by more long-term (6 years), but less intensive, monitoring (Ulén et al. 2018). The low turbidity

(measured *in situ*) and TOC (from flow-proportional sampling) in 2013/2014 in the present study (Table 2) support the finding that improved aggregate stability can develop after structure liming (Ulén et al. 2018). Consequently, less particulate matter and organic matter are detached from soil aggregates by rain. Low CNO_3N under fallow (2012/13), when the soil was not fertilised or tilled, was anticipated, since such soil can be expected to have a low mineral N content. This, and the significantly lower CNO_3N-Q slope than in the three other cropping systems, confirmed findings in adjacent experimental plots of significantly low NO_3N leaching from fallow (Svanbäck et al. 2014). At the same time, there was relatively high PP transport from the experimental plots under fallow, possibly because there were more vertically oriented macropores in fallow soil than in ploughed soil and the macropores were also better connected (Hellner et al. 2018). In general, high variability in turbidity relative to Q for fallow (CV_T/CT_Q) was observed in the present study. Hence soil under fallow does not generally hamper transport of particles and associated P with macropore flow.

A sampling strategy with frequent subsampling to obtain composite samples relies on a relatively synchronised C–Q relationship. Thus load estimation based on flow-proportional sampling during periods with a long residence time can potentially be of lower precision. In the present study, the sampling strategies with *in situ* measurement of NO_3N and with frequent subsample collection to obtain a mixed composite sample for laboratory analysis gave reasonably similar NO_3N leaching. Calibration of SS from turbidity values requires more effort, since the relationship is non-linear and requires manual sampling in events.

Turbidity has been used previously as a surrogate for TP concentrations (CTP) (e.g. Jones et al. 2011), but was tested here as a surrogate for PP concentrations, based on the observation that the proportion of DRP in TP varies seasonally (Ulén et al. 2012). The differing pattern of CDRP and TURB in early spring suggests that DRP was not solely derived from desorption from fine particles in water, but also from the hydroxy-aluminum layer of vermiculite. The direct role of pH in such P desorption is complicated, and a clear relationship has only been reported at low pH (Eriksson 2016) corresponding to a lower level than usually prevailing during snowmelt at the present site. However, the relatively high proportion of DRP in TP leached in spring 2012 supports earlier findings of generally higher losses of dissolved forms of P and glyphosate in spring than in autumn (Ulén et al. 2012).

Soil tillage, soil organic matter content, and manure load are well-known explanatory factors for CNO3N in

drainage water from agricultural areas, beside hydro-climatological factors and artificial drainage (e.g. Dinnes et al. 2001). Manure load and mineralisation of soil N, triggered by tillage, are sometimes excluded from C–Q assessments of agricultural catchments. However, this could be a source of error, since enhanced C_{NO3N} and 'hot moments' in NO_3N leaching have been demonstrated when a drained field was irrigated with diluted pig slurry (Liu, Youssef, et al. 2020). The same study also demonstrated that CNO_3N-Q was affected by tillage. In the present study, the significantly steeper CNO_3N-Q slopes could be attributed to tillage and digging the soil after terminating a fallow and improving the drainage (2013).

More knowledge is needed about non-linear C–Q relationships in small fields. Very long-term studies are needed when assessing changes in agricultural and soil management practices, especially when a narrow time-window in the hydrological years is used. Understanding the spatial variation in groundwater residence times is essential, both at the field scale and in larger spatial domains. Fine-tuned monitoring of soil should be encouraged in order to improve assessment/modelling results based on high-frequency water quality monitoring.

The present assessment did not statistically verify a change in P leaching after combined changes in soil and drainage management. However, it indicated that sensor equipment for high-frequency P measurements can be useful in assessing P leaching processes, especially in cold-climate regions where freeze–thaw processes contribute to P mobilisation and to changes in P interactions with soil (Liu et al. 2019). High-frequency long-term monitoring data for fields where direct effects of agricultural management practices can be observed, and where there is no input from sewage water, could be especially useful.

Acknowledgements

Disclosure statement

Funding

Notes on contributor

Barbro Ulén is professor emerita in Water Quality Management at the Swedish University of Agricultural Sciences. Her research interests include eutrophication and mitigation of non-point source losses of plant nutrients from arable land.

ORCID

Barbro Ulén http://orcid.org/0000-0002-7988-3584

References

Bauwe A, Tiemeyer B, Kahle P, Lennartz B. 2015. Classifying hydrological events to quantify their impact on nitrate leaching across three spatial scales. J Hydrol. 531:589–601. DOI:10.1016/j.hydrol.2015.10.069.

Blaen PJ, Khamis K, Loyd C, Corner-Werner S, Ciocca F, Thomas RM, MacKenzie AB, Krause S. 2017. High-frequency monitoring of catchment nutrient exports reveals highly variable storm event responses and dynamic source zone activation. J Geophys Res Biogeosci. 122:2265–2381. DOI:10.1002/2017JG003904.

Dinnes DL, Karlen DL, Jaynes DB, Kaspar TC, Hatfield JL, Colvin TS, Cambardella CA. 2001. Nitrogen management strategies to reduce nitrate leaching in tile-drained midwestern soils. Review and Interpretation. Agron J. 94:153–171.

Duncan JM, Welty C, Kemper JT, Groffman PM, Band LE. 2017. Dynamics of nitrate concentration-discharge patterns in an urban watershed. Water Resour Res. 53:4349–4365. DOI:10.1002/2017WR020500.

ECS. 1996. European Standard EN 1189 water quality. Determination of phosphorus. Ammonium-molybdate spectrometric method. Brussels: European Committee for Standardization, 18 pp.

Egnér H, Riem H, Domingo WR. 1960. Studies on chemical soil analysis as the basis for estimating soil fertility. II Chemical extraction methods for phosphorus and potssium determination. Kungl Lantbrukshögskolans Annaler. 26:199–215.

Eludoyin AO, Griffith B, Orr RJ, Bol R, Quine TA, Brazier RE. 2017. An evaluation of the hysteresis in chemical concentration-discharge (C-Q) relationships from drained, intensively managed grasslands in southwest England. Hydrol Sci J. 62:1243–1254. DOI:10.1080/02626667.2017.1313979.

Eriksson A-K. 2016. Phosphorus speciation in Swedish agricultural clay soil – influence of fertilisation and minerology. Doctoral thesis 2016:25, Acta Universitatis. Agriculturae Sueciae, Faculty of Natural Resources and Agricultural Sciences, Swedish University of Agricultural Sciences.

Flury M. 1996. Experimental evidence of transport of pesticides through field soils – a review. J Environ Qual. 25:25–45. DOI:10.2134/jeq199600472425002500010005x.

Gramlich A, Stoll S, Stamm C, Walter T, Prasuhn V. 2018. Effects of artificial land drainage on hydrology, nutrient and pesticide fluxes from agricultural fields – a review. Agric Ecosys Environ. 266:84–99. DOI:10.106/j.agee.2018.04.005.

Hellner Q, Koestel J, Ulén B, Larsbo M. 2018. Effects of tillage and liming on macropore networks derived from X-ray tomagrophy images of a silty clay soil. Soil Use Manage. 34:197–205. DOI:10.1111/sum12418.

Holloway JM, Dahlgren RA, Hansen B, Casey WH. 1998. Contribution of bedrock nitrogen to high nitrate concentrations in stream water. Nature. 395:785–788. DOI:10.1038/27410.

ISO. 1996. International Organization for Standardization, ISO 13395. Water quality – determination of nitrite nitrogen and nitrate nitrogen and the sum of both by flow analysis (CFA and FIA) and spectrometric detection. [accessed 2019 December 11]. https://www.iso.org.

ISO. 2003. International Organization for Standardization. ISO 15681-1:2003. Water quality – determination of phosphate and total phosphorus by flow analysis (CFA and FIA) Part I methods for flow injection analysis (FIA). [accessed 2019 December 11]. https://www.iso.org.

ISO. 2005. International Organization for Standardization. ISO 11732. Water quality – determination of ammonium nitrogen. Method by flow analysis (CFA and FIA) and spectrometric detection. [accessed 2019 December 11]. https://www.iso.org.

Jones AS, Stevens DK, Horsburgh JS, Mesner NO. 2011. Surrogate measures for providing high frequency estimates of total suspended solids and total phosphorus. J Am Water Resour Assoc. 42:239–353.

Kämäri M, Tattari S, Lotsari E, Koskiaho J, Lloy CEM. 2018. High-frequency monitoring reveals seasonal and event-scale water quality variation in a temporally frozen river. J Hydrol. 564:619–639. DOI:101016/j.jhydrol.2018.07.037.

Knapp JLA, von Freyberg J, Studer B, Kiewiet L, Kirchner JW. 2020. Concentration-discharge relationships vary among hydrological events, reflecting differences in event characteristics. Hydrol Earth Sys Sci. DOI:10.5194/hess-2019-684.

Liu J, Baulch HM, Macrae ML, Wilson HE, Elliot JA, Bergström L, Glenn AJ, Vadas PA. 2019. Agricultural water quality in cold climates: processes, drivers, management options and research needs. J Environ Qual. 48:792–802. DOI:10-2134/jeq2019.05.0220.

Liu W, Maxwell B, Brigand F, Youssef M, Chescscheir G, Tian S. 2020. Multipoint high-frequency sampling system to gain deeper insights on the fate of nitrate in artificially drained fields. J Irrig Drain Engng. 146(1). DOI:10.1061/(ASCE)R1943-4774.0001438.

Liu W, Youssef M, Brigand F, Chescscheir G, Tian S, Maxwell B. 2020. Processes and mechanisms controlling nitrate dynamics in an artificially drained field: insights from high-frequency water quality measurements. Agric Water Manage. 232. DOI:10.1016/j.agwat2020.10603.

Lloyd CEM, Freer JE, Johnes PJ, Collins AL. 2016a. Using hysteresis analysis of high-resolution water quality monitoring data, including uncertainty to infer controls on nutrient and sediment transfer in catchments. Sci Tot Environ. 543:388–404. DOI:10.1016/j.scitotenv.2015.11.028.

Lloyd CEM, Freer JE, Johnes PJ, Collins AL. 2016b. Technical note: testing an improved index for analysing storm discharge-concentration hysteresis. Hydrol Earth Syst Sci. 20:625–632. DOI:10.5194/hess-20-625-2016.

Outram FN, Cooper RJ, Sünnenberg G, Hiscock KM, Lowett AA. 2016. Antecedent conditions, hydrological connectivity and anthropogenic inputs: factors affecting nitrate and phophorus transfer to agricultural headwater streams. Sci Tot Environ. 545–546:184–199. DOI:10.1016/j.scitotetenv.2015.12.0250048-9697.

Penn CJ, Mullins GL, Zelazny LW. 2005. Mineralogy in relation to phosphorus sorption and dissolved phosphorus losses in runoff. Soil Sci Soc Am J. 69:1532–1540. DOI:10.2136/ssaj/2004.0224.

Ryden JC, Syers JK, Harris RF. 1974. Phosphorus in runoff and streams. Adv Agron. 25:1–25. DOI:10.1016/s0065-2113(08)6077-4.

Scherer HW. 1993. Dynamics and availability of the non-exchangeable NH_4-N – a review. Eur J Agron. 2:149–160. DOI:10.1016/S1161-0301(14)80129-x.

Simonsson M, Adediran G, Aronsson H, Etana A, Gustafsson JP, Hillier S, Lundberg H. 2019. Phosphorus-bearing particles in lechate from agricultural soils. Goldschmith2019 Abstract, Barcelona 18-23 August, 2019. [accessed 2019 December 11]. https://www.goldschmidt.info.

SMHI. 2019. Swedish Meteorological and Hydrological Institute. Open climate data [accessed 2019 November 10]. https://www.smhi.se/klimatdata.

Svanbäck A, Ulén B, Etana A. 2014. Mitigation of phosphorus leaching losses via subsurface drains from a cracking marine clay soil. Agric Ecosys Environ. 184:124–134. DOI:10.1016/j.agee.2013.11.017.

Thompson SE, Basu NB, Lascurain J, Aubeneau A, Rao PSC. 2011. Relative dominance of hydrologie versus biogeochemical factors on solute export across impact gradients. Water Resour Res. 47:1–20. DOI:10.1029/2010WR009605.

Ulén B, Alex G, Kreuger J, Svanbäck A, Etana A. 2012. Particulate-facilitating leaching of glyphosate and phosphorus from a marine clay soil via tile drains. Acta Agric Scand B Soil and Plant. 62(Suppl. 2):241–251. DOI:10.1080/09064710.2012.697572.

Ulén B, Geranmayeh P, Blomberg M, Bieroza M. 2019. Seasonal variation in nutrient retention in a free water surface constructed wetland monitored with flow-proportional sampling and optical sensors. Ecol Eng. 139:Article 105588. DOI:10.1016/j.ecoleng.2019.105588.

Ulén B, Larsbo M, Kreuger J, Svanbäck A. 2014. Spatial variation in herbicide leaching from a marine clay soil via subsurface drains. Pest Manage Sci. 70:405–414. DOI:10.1002/ps3574.

Ulén B, Larsbo M, Koestel J, Hellner Q, Blomberg M, Geranmayeh P. 2018. Assessing strategies to mitigate phosphorus leaching from drained clay soils. Ambio. 47(Suppl. 1):114–123. DOI:10.1007/s13280-017-0991-x.

Vaugham MCM, Bowden WB, Shanley JB, Vermileya A, Sleeper R, Gold AJ, Pradhanang SM, Inamdar SP, Levia DF, Andres AS, et al. 2017. High-frequency dissolved organic carbon and nitrate measurements reveal differences in storm hysteresis and loading in relation to land cover and seasonality. Water Resour. Res. 53:5345–5363. DOI:10.1002/2017WR020481.

Zimmer MA, Pellerin B, Burns DA, Petrochenkov G. 2018. Temporal variability in nitrate-discharge relationships in large rivers as revealed by high-frequency data. Water Resour Res. 55:1–17. DOI:10.1029/2018WR023478.